Q. J. R. Meteorol. Soc. (2002), **128**, pp. 1059–1073

Extratropical low-frequency variability as a low-dimensional problem. II: Stationarity and stability of large-scale equilibria

By FABIO D'ANDREA*

École Normale Supérieure, Paris, France

(Received 24 July 2000; revised 23 January 2002)

SUMMARY

Stationarity and stability properties of large-scale persistent anomalies in the northern hemisphere are addressed. The low-order model developed in Part I is used for this purpose. It was obtained as the projection of a three-level quasi-geostrophic system on the ten leading empirical orthogonal functions. Three global quasi-stationary states are identified, which represent the Arctic high and the positive and negative phases of the main teleconnections (Pacific North American and North Atlantic oscillation). The quasi-stationary solutions have only a partial correspondence to the weather regimes found in Part I. Stability analysis shows a growing mode that describes an oscillation between the two phases of the teleconnections. The negative teleconnection state is also shown to be much more stable than the other two. Possible decay mechanisms are also discussed.

KEYWORDS: Extratropical circulation Low-order modelling

1. INTRODUCTION

Weather regimes are defined as recurrent and/or persistent patterns of variability of the extratropical circulation at the intraseasonal time-scale. They are normally diagnosed by some form of multivariate statistical analysis (e.g. probability density estimations or cluster analysis) in attempts to find the most probable states in the phase-space of a given observed or modelled atmospheric variable. From the theoretical point of view, it has been hypothesized that they may be the result of the existence of multiple fixed points in the governing equations of the large-scale flow. This hypothesis in its present form dates back to the work of Charney and DeVore (1979), and was later reformulated more explicitly by Reinhold and Pierrehumbert (1982). This identification of regimes with large-scale equilibria may not be trivial. Michelangeli *et al.* (1995) argued that, in the case of an observational regional study, the regimes defined by cluster analysis are not necessarily equivalent to stationary states. They compared the regimes obtained from that method with the regimes obtained by a statistical equilibration of the large-scale part of the flow. The two sets of regime patterns were largely, but not entirely, coincident. In an attempt to reconcile statistics and dynamics, Marshall and Molteni (1993) proposed the use of neutral vectors, or the singular vectors of the linearized equation having the smallest growth rate. This approach has, nevertheless, the disadvantage of being based on a number of ad hoc hypotheses, not least that of linearity. A nonlinear approach (Haines and Hannachi 1995; Hannachi 1997) found a better coincidence between regimes and equilibria in the framework of a General Circulation Model (GCM). In the cited works, the authors compared the regimes defined by some form of cluster analysis on the model output with the stationary solution of the barotropic potential-vorticity equation in the subspace of the leading empirical orthogonal functions (EOFs) of the GCM.

The approach used in this paper is similar to that of Haines and Hannachi (1995) and Hannachi (1997), but with the advantage that the equilibria of the equations and the clusters correspond to the same model. Another difference with the above quoted works is that the domain in which the analysis is carried out is the entire northern

* Corresponding address: Laboratoire de Météorologie Dynamique, École Normale Supérieure, 24 Rue Lhomond, 75005 Paris, France. e-mail: dandrea@lmd.ens.fr

hemisphere; this is made possible by the use of the low-dimensional model with flow-dependent parametrization of the eddy forcing, developed in D'Andrea and Vautard (2001, hereafter Part 1). In Part 1, a simplified model of the quasi-geostrophic (QG) dynamics was built within a low-dimensional space by projecting the equation of an intermediate complexity model on its ten leading EOFs. This low-dimensional model allows a systematic search for stationary solutions that can be compared to the weather regimes obtained in Part I, as well as a stability analysis of these solutions.

The aim of this work is to investigate further the hypothesis that weather regimes are related to fixed points in the equations of the dynamics. In section 2 a brief discussion of the results of Part I is presented. In section 3 stationary solutions to the model equations are calculated and compared to the weather regimes defined by the statistical analysis of Part 1. The use of the low-order model also allows some consideration of the stability of the regimes and the transitions between them. This is done in section 4 by linear stability analysis of the stationary solutions found in section 3. This analysis also reveals an oscillatory behaviour in the vicinity of the stationary solutions. Section 5 contains a general discussion and conclusions.

2. The low-order model

The three-level model of Marshall and Molteni (1993), based on the QG potential-vorticity equation, was used in Part I to show that the low-frequency variability is basically a low-dimensional problem. At each level the model equations are:

$$\frac{\partial q}{\partial t} = -\mathrm{J}(\psi, q) - D(\psi) + S, \tag{1}$$

where J represents the Jacobian operator, and ψ is the QG stream function linked to the QG potential vorticity, q, by a relation $q = \mathcal{L}\psi$. The linear dissipation term, D, includes in a simple way the Ekman dissipation (orography dependent) and a Newtonian relaxation between the layers. The orographic contribution to the potential vorticity at the lower layer is included in the operator $\mathcal{L}$. The constant with time, but spatially varying, forcing term S is designed to include the sources of potential vorticity that result from processes not explicitly included in the equations. This model possesses a realistic climatology, including stormtracks and low-frequency variability structures.

The low-dimensional model, designed to simulate only the low-frequency part of the QG model dynamics, is based on two fundamental ideas: (i) the choice of an optimal orthogonal basis for projecting the equations; and (ii) the construction of a closure term to represent the effect of the neglected scales. The optimal basis of the low-order phase space is simply composed of the leading ten EOFs of the reference model. The problem of closure is solved by parametrizing the effect of the baroclinic transients, which are known to be crucial for the maintenance of the low-frequency variability. This parametrization is obtained via the method of analogues, in this case a statistical model based on a look-up table that uses the large-scale flow as a predictor and the simplified model tendency error as predictands. The low-dimensional model equation can be written:

$$\frac{\partial q'}{\partial t} = -\widehat{\mathrm{J}}(\psi', q') - \widehat{D}(\psi') + S'(\psi'), \tag{2}$$

where the primes are used to remind us that the fields q, ψ and S are truncated to the first ten EOFs. Note that these fields are three-dimensional, since the EOFs were calculated on the three vertical model levels at the same time. The operator $\widehat{\mathrm{J}}$ is the

TABLE 1. VALUES OF $\|\frac{\partial \psi}{\partial t}\|$ AT THE THREE QUASI-STATIONARY STATES OF THE LOW-ORDER MODEL

State	$\left\|\frac{\partial \psi}{\partial t}\right\|$ ($m^2 s^{-2}$)
Arctic High	0.11
Positive Teleconnection	2.94
Negative Teleconnection	1.62

bilinear form that represents the application of the Jacobian to the three vertical levels, while $\widehat{D}$ is the linear dissipation on the three levels. The low-order model was shown to have the same climatology and low-frequency variability as the reference model. The comparison between the two models was based on the mean and variance in the low-frequency band, and on weather regimes. These regimes were defined by a cluster analysis method (Michelangeli *et al.* 1995); see Part I for details.

3. MULTIPLE EQUILIBRIA IN THE SIMPLIFIED MODEL

In this section the global equilibria of the low-dimensional model defined in Part 1 are obtained as stationary solutions of Eq. (2). These equilibria are then compared to the regimes obtained in Part 1.

(*a*) *Quasi-stationary states*

In order to find the equilibrium points of the low-order model, the squared Euclidean norm of the stream function tendency, derived from Eq. (2), is minimized. A quasi-Newton algorithm is used to find the minima. This algorithm requires the knowledge of the gradient of the function at given points, which is readily computed by differentiating Eq. (2) ; note that the formulation of the closure term $S'(\psi')$ in Eq. (2) is differentiable (see definition in Eq. 8 of Part I). To obtain reliable solutions, a large number of initial states from the reference model integration have been used in the minimization, and several local minima were obtained.

In order to compare the values of the tendency function at the local minima, the distribution of the tendency norms of the reference integration has been considered. The norm was computed after truncation to the first ten EOFs. This distribution has a mean value of 22.6 $m^2 s^{-2}$, a standard deviation of 10.6 $m^2 s^{-2}$ and a minimum of 3.9 $m^2 s^{-2}$. The tendency of the mean state of the model is 5.4 $m^2 s^{-2}$.

Only the local minima in which the value of the tendency function norm was lower than the minimum value of this distribution were retained. In the end three different states were found by this procedure. The tendency does not exactly vanish at these points, but its residual is very small; they can thus be called quasi-stationary states. The values of the norm of the tendency function for these three quasi-stationary solutions appear in Table 1.

The total and anomaly fields of the quasi-stationary states are shown in Fig. 1. The first state, upper panels of Fig. 1, which will be called *Arctic High*, shows a strong weakening of the meridional gradient of the total stream function field, especially over the Atlantic and Pacific oceans. The other two anomaly states are approximatively opposite to each other, and represent respectively the positive phases of the North Atlantic Oscillation (NAO) and the Pacific North American (PNA; central panels), and

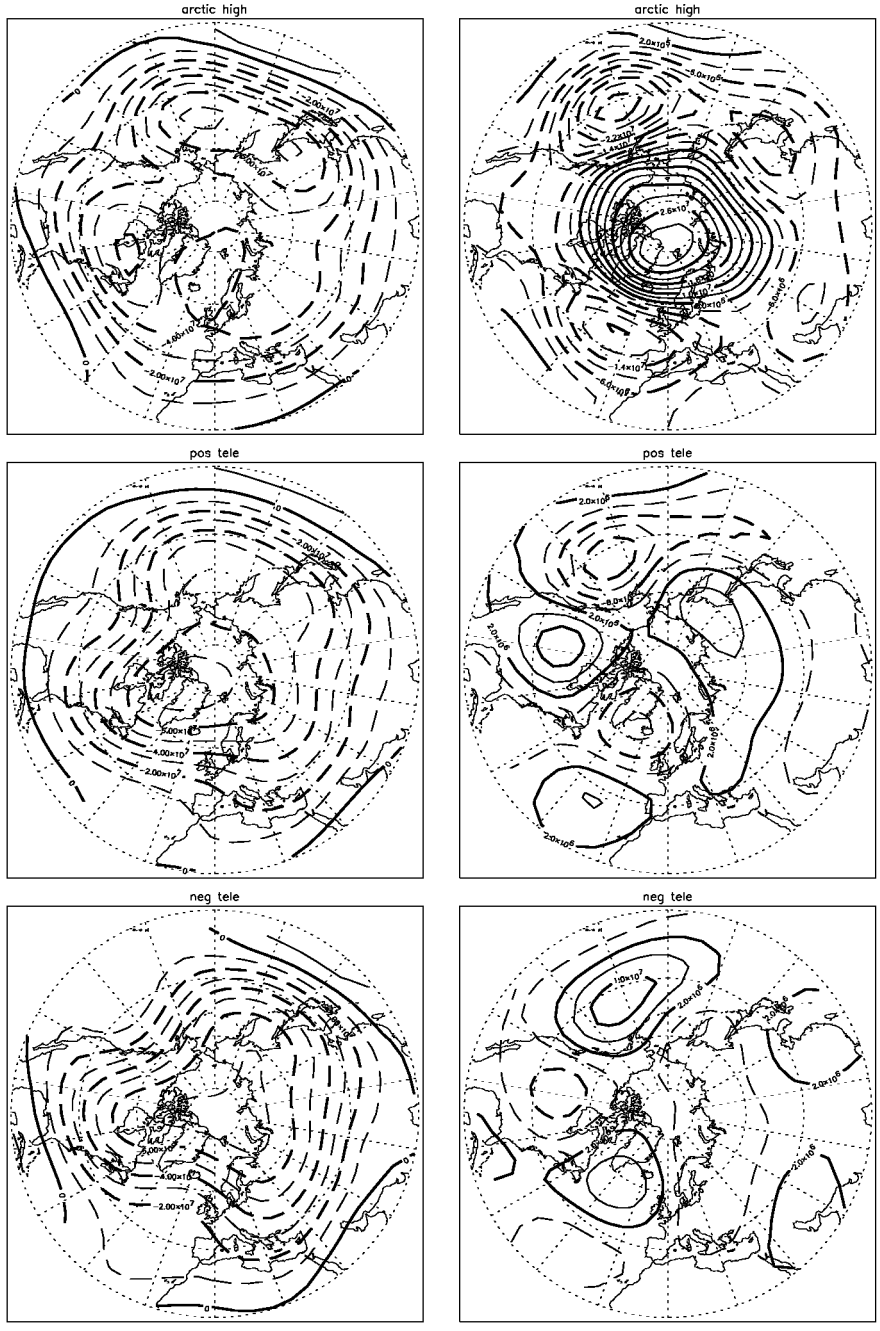

Figure 1. Full (left-hand column) and anomaly (right-hand column) stream function field of the quasi-stationary states of the low-order model at the 500 hPa level. Contours every 4×10^6 $m^2 s^{-1}$, negative contours dashed. From top to bottom: Arctic High, Positive Teleconnection and Negative Teleconnection state.

their opposite (bottom panels). These two states will be called *Positive* and *Negative Teleconnections*.

Figure 2 shows the contribution of the different terms in the balance equation for the equilibria representing, respectively from top to bottom, advection, dissipation, forcing, and residual tendency. The contributions are shown after subtraction of their mean; they are consequently anomalous tendency terms.

For the Arctic High (left-hand column of Fig. 2), it is clear that advection tends to maintain the anomaly over the pole against dissipation. Over the Atlantic Ocean the anomalous forcing, on the other hand, appears to create the negative anomaly, it pushes the area of high meridional gradient towards the north and displaces the jet towards the south. It seems that in the Atlantic sector, the transients are important for maintaining the reduced zonal flow. In the other two cases the anomalous tendency terms are smaller than in the Arctic High case. All the terms are close to the climatology. The Negative Teleconnection state projects on the negative NAO with a weakening of the westerlies over the Atlantic, but in this case the transient forcing has a rather opposite contribution with respect to the Arctic High case. The Positive and Negative Teleconnection quasi-stationary solutions have large residuals that have the same order of magnitude of the anomalous tendencies. Their residuals have a similar pattern, because both of them project on the last basis vector (compare Fig. 2 of Part 1). In the case of the Arctic High on the other hand the anomalies are also in equilibrium.

(*b*) *Quasi-stationary solutions and clusters*

In this section, the correspondence between quasi-stationary states and weather regimes as defined in Part 1 will be examined. The question that needs to be answered is whether the regimes of the low-order model can be explained as the effect of global equilibria.

Figure 1 should be compared with Figs. 6 and 7 of Part 1. From a visual inspection, it is evident that this correspondence is only approximate. It should be borne in mind that the quasi-equilibrium states are model states, defined on the whole globe and on the three model levels, while the clusters are hemispheric and defined at 500 hPa.

Here the comparison is made in terms of ACC (anomaly correlation coefficient) and of RMS (root-mean-square) difference between the northern hemisphere part of the quasi-stationary states (Fig. 1) and the clusters of Fig. 6 of Part 1. The best correspondences were found between:

(i) the Arctic High state and cluster 1;
(ii) the Negative Teleconnection state and cluster 5;
(iii) the Positive Teleconnection state and cluster 4.

The scores are listed in Table 2.

The zonally symmetric structure of both the Arctic High and cluster 1 is responsible for the high ACC score, while the strong difference in amplitude gives a high RMS error.

The Negative Teleconnection state and cluster 5 have a good score in both measures.

The case of the Positive Teleconnection state is somewhat more delicate. The NAO pattern over the Atlantic ocean is found in the fourth cluster. The rest of the pattern, however, does not resemble it very much, and the hemispheric ACC and RMS errors are rather poor. It could be that the regime corresponds to the stationary state in the Atlantic sector only, and the Pacific part may simply not be found by the cluster analysis because its higher instability makes it more transient. This conclusion may seem arbitrary at this point but its soundness will be shown below, when the linear stability of this state is analysed.

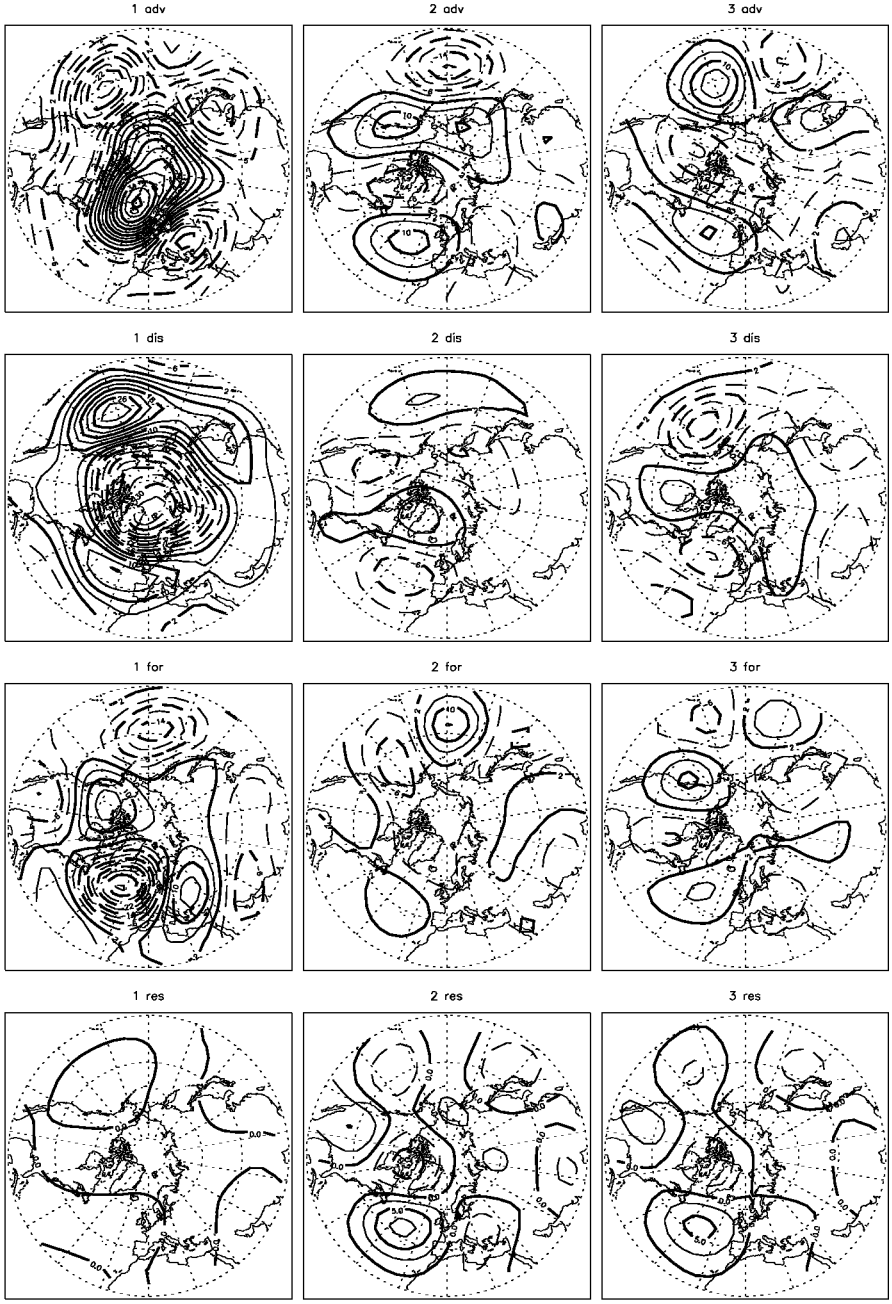

Figure 2. Balance of anomalous stream function tendency terms for the three quasi-stationary solutions at 500 hPa. Left- to right-hand columns: Arctic High, Positive Teleconnections and Negative Teleconnections. Top to bottom: anomalous advection term $J(\psi, q) - \overline{J(\psi, q)}$, dissipation term $D(\psi) - \overline{D(\psi)}$, forcing term $S(\psi) - \overline{S(\psi)}$ and residual. Contours are every 4 $m^2 s^{-2}$. See text for details.

TABLE 2. COMPARISON OF THE QUASI-STATIONARY SOLUTION OF FIG. 1 AND THE WEATHER REGIMES DEFINED BY CLUSTER ANALYSIS OF FIG. 7 OF PART 1

	Arctic High–cluster 1	Positive Teleconnection–cluster 4	Negative Teleconnection–cluster 5
ACC	0.89	0.29	0.75
RMS	0.23	0.10	0.04

The RMS error is normalized by the norm of the mean state of the model (Fig. 4(a) of Part 1).

In summary, the link between regimes of the time evolution and stationary states of the flow is not trivial. Two of the quasi-stationary states can be roughly identified with the results of cluster analysis, and a third only in part. The other two clusters of Fig. 7 of Part 1, on the other hand, are not found. Many studies (e.g. Kimoto and Ghil 1993) have suggested that weather regimes should be regarded as recurrent regional phenomena. Global equilibria may then be linked to them in an indirect way, e.g. creating the synoptic situations favourable to the inception or maintenance of a given regime. This hypothesis may explain the imperfect correspondence, and will be discussed again in the last section.

The stability of the quasi-stationary solutions will be assessed in the following section. This enables us to understand the dynamics of the low-order model, but it will be seen that it also allows some more consideration on the link between weather regimes and global equilibria.

4. STABILITY OF THE QUASI-STATIONARY SOLUTIONS

A linear stability analysis of the quasi-stationary solutions found above is carried out in this section. In a standard procedure, the low-order model is linearized around its three quasi-stationary states and its Jacobian matrix is diagonalized. An eigenvalue, λ, with a positive real part indicates a perturbation growth, whose rate (e-folding time) is given by $1/\mathrm{Re}(\lambda)$. If the eigenvalue has a non-zero imaginary part, then the perturbation growth is oscillatory, and its period of oscillation is given by $2\pi/\mathrm{Im}(\lambda)$. The real and imaginary parts of the corresponding eigenvectors give the phases of the oscillation, at 1/4 period phase lag from each other.

(*a*) *Arctic High*

The linearization around the Arctic High state gives three conjugate pairs of complex eigenvalues with positive real parts, i.e. three directions of instability. The growth rate of these unstable directions and their oscillation periodicities are listed in Table 3.

The most unstable direction has an e-folding time of 9 days and a period of oscillation of 13 days. Its real and imaginary parts at 500 hPa are shown in Figs. 3(a) and (b). Over the North Pacific, the patterns resemble an eastward propagating Rossby wave. The eastward propagation can be confirmed when conducting a long integration of the linearized model by re-normalizing the perturbation in the course of the integration, until a limit cycle is established (not shown). Analysis of the other vertical levels of the model (not shown) shows that this Rossby wave has an equivalent barotropic vertical structure. This means that the Arctic High regime is destabilized by a barotropically unstable perturbation propagating eastward from the Asian continent.

(*b*) *Positive Teleconnection*

Two pairs of eigenvectors with positive real parts are obtained and shown in Table 4. The most unstable eigenvector closely resembles the first eigenvector of the Arctic High

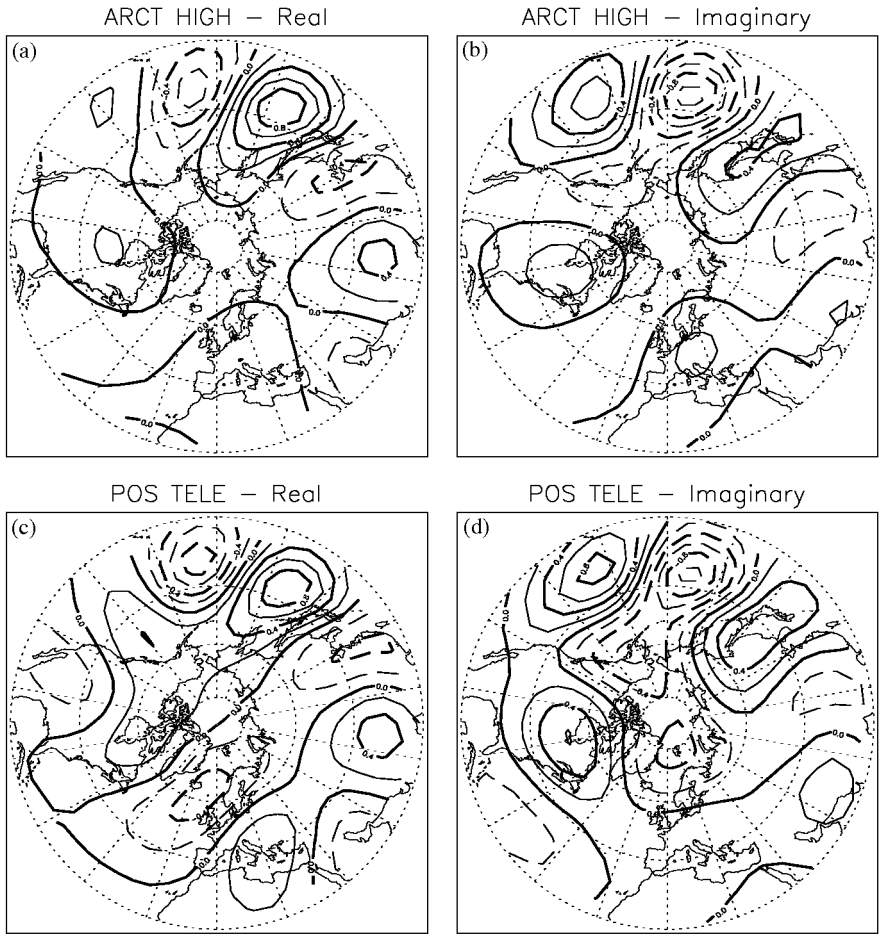

Figure 3. (a) and (b): real and imaginary part of the first eigenvector, expressed as stream function tendency, of the low-order model linearized around the Arctic High state. Only the 500 hPa part is shown; (c) and (d) similar but for the Positive Teleconnection. Vectors are normalized by the *sup* norm, contours every 0.2 $m^2 s^{-2}$.

state. Its real and imaginary parts are shown in Figs. 3(c) and (d). In this case a longer e-folding time is found, but the periodicity, which gives the phase speed of the Rossby wave, is comparable to that of the Arctic High. The spatial patterns are also very similar. This instability is mainly concentrated in the Pacific region, and causes the decay of the negative anomaly that both the Arctic High and the Positive Teleconnection states have in that region.

Going back to the problem of similarity between the Positive Teleconnection state and weather regime four of Fig. 7 of Part 1, this pattern of instability can explain why the weather regime is identifiable to the quasi-stationary state only over the Atlantic region. The Atlantic part of the quasi-stationary state is in fact more stable than the Pacific part, and the main amplitude of the tendency residual of Fig. 2 acts in a stable region. A simple verification of this point can be obtained by observing the low-order model evolution when started from this quasi-stationary state. The first 55 days of evolution are reported in Fig. 4. It can be seen that the NAO anomaly is stationary in phase, yet

TABLE 3. SUMMARY OF THE LINEAR STABILITY OF THE ARCTIC HIGH STATE

Couple	e-folding time (days)	Period (days)
1	8.9	13.3
2	67.0	73.9
3	153.3	29.7

The e-folding time is defined as $1/\mathrm{Re}(\lambda)$ and period as $2\pi/\mathrm{Im}(\lambda)$ where λ is the eigenvalue. Only the unstable part of the eigenvalue spectrum is listed.

TABLE 4. AS TABLE 3 BUT FOR THE POSITIVE TELECONNECTIONS STATE

Couple	e-folding time (days)	Period (days)
1	25.7	17.0
2	434.6	82.9

increasing in amplitude, and is recognizable until around days 45–50, while the Pacific part of the flow is destabilized towards days 25–30. The cluster analysis used to define the weather regime only selects the most stationary part of this state.

Note also that the increase in amplitude of the NAO pattern can be interpreted as an effect of the residual tendency (compare Fig. 2 bottom central panel and Fig. 4).

(*c*) *Negative Teleconnection*

The Negative Teleconnection state has only one conjugate pair of positive real-part eigenvalues, as can be seen in Table 5. The real and imaginary parts of the eigenvector are shown in Figs. 5(a) and (b). The pattern in Fig. 5(b) precedes the pattern in Fig. 5(a) by 1/4 period in phase. This eigenvector describes an oscillation (with a low growth rate) that propagates westward. The two phases of the oscillation that are marked by the two signs of the real part of the eigenvector resemble closely the positive and negative phases of the NAO respectively. This behaviour suggests the existence in the model of a mode of oscillation between the Positive and Negative Teleconnection states, at least in their North Atlantic part. This oscillation has a period of approximatively 46 days.

It is interesting to note that an oscillation similar to this is also found as the second unstable eigenvector in the analysis of the Positive Teleconnection state, although with a different period (see Table 4). The real and imaginary parts of the eigenvector are also shown in Figs. 5(c) and (d). This tends to confirm the suggestion of an oscillation between the two states.

Again, the behaviour of the model around the quasi-stationary state can be directly observed by an integration of the low-dimensional (nonlinear) model. The first 55 days, starting from the Negative Teleconnection state are shown in Fig. 6. A whole oscillation can be seen, with period in the range 50–55 days. At days 20–25 the opposite phase of NAO is recognizable, similar to the Atlantic part of the Positive Teleconnection state or to regime 4 of Fig. 6 of Part 1.

Simmons *et al.* (1983) also found an oscillating eigenvalue in a linear stability analysis of the mean flow. Their oscillation also had two opposite phases that resembled an NAO pattern, and was seen at the time as a possible mark of the low-frequency alternation between regimes. Although it is common practice, one should probably use

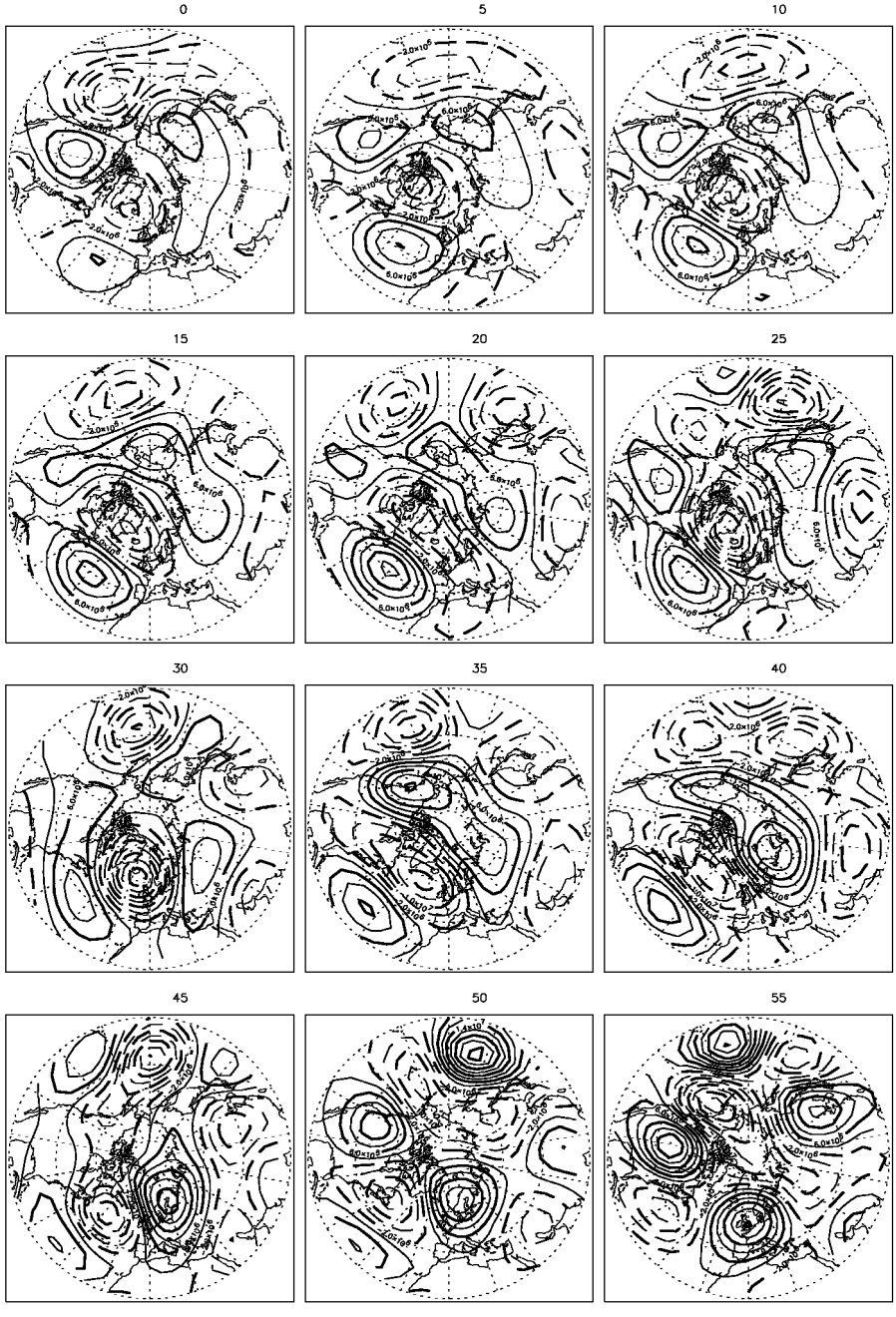

Figure 4. Time evolution of the Positive Teleconnection. Anomalies of the stream function at 500 hPa with contours every 4×10^6 $m^2 s^{-1}$. Above each panel the day of integration is given.

TABLE 5. AS TABLE 3 BUT FOR THE NEGATIVE TELECONNECTIONS STATE

Couple	e-folding time (days)	Period (days)
1	86.7	46.3

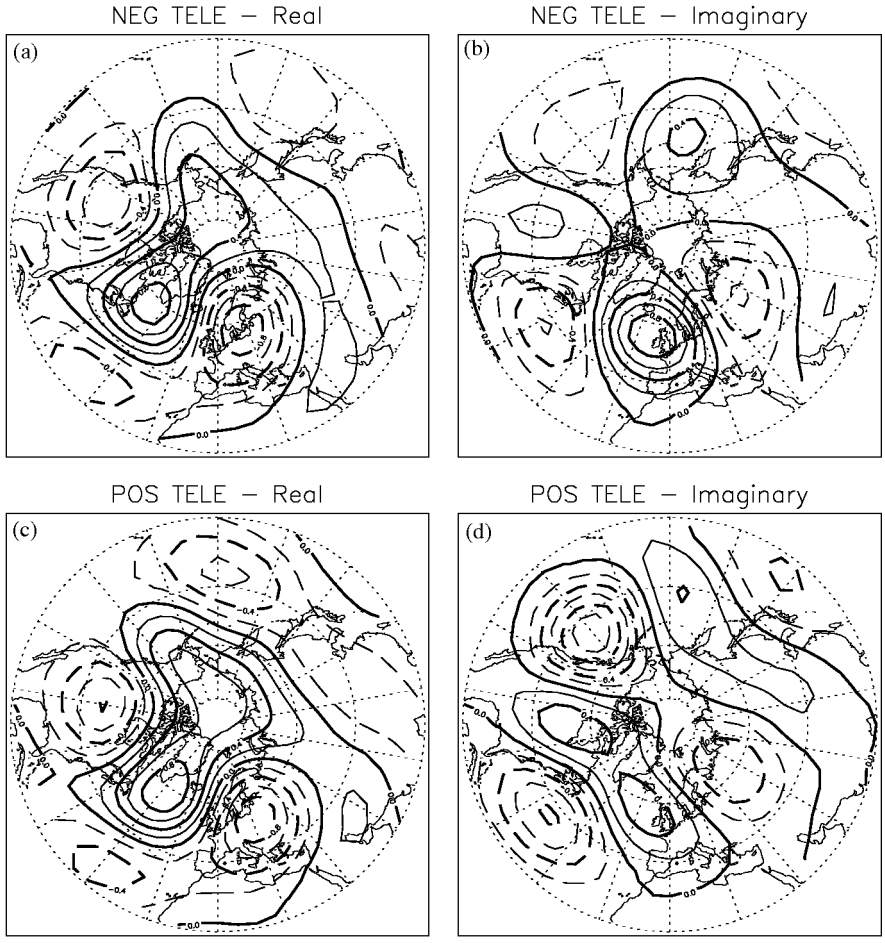

Figure 5. Same as Fig. 3 but (a) and (b) are for the first eigenvector of the linear stability analysis of the Positive Teleconnection, and (c) and (d) are for the second eigenvector of the Negative Teleconnection. See text for details.

the linearization of model equations around the mean state with some caution. The mean is not a stationary (nor a quasi-stationary) state of the circulation. In the case of this paper, the linearization is performed around states that are as close as possible to stationarity, so one may reasonably believe that the system actually behaves almost linearly in their neighbourhoods, as is confirmed by the integration of the complete nonlinear model in Fig. 4 and Fig. 6.

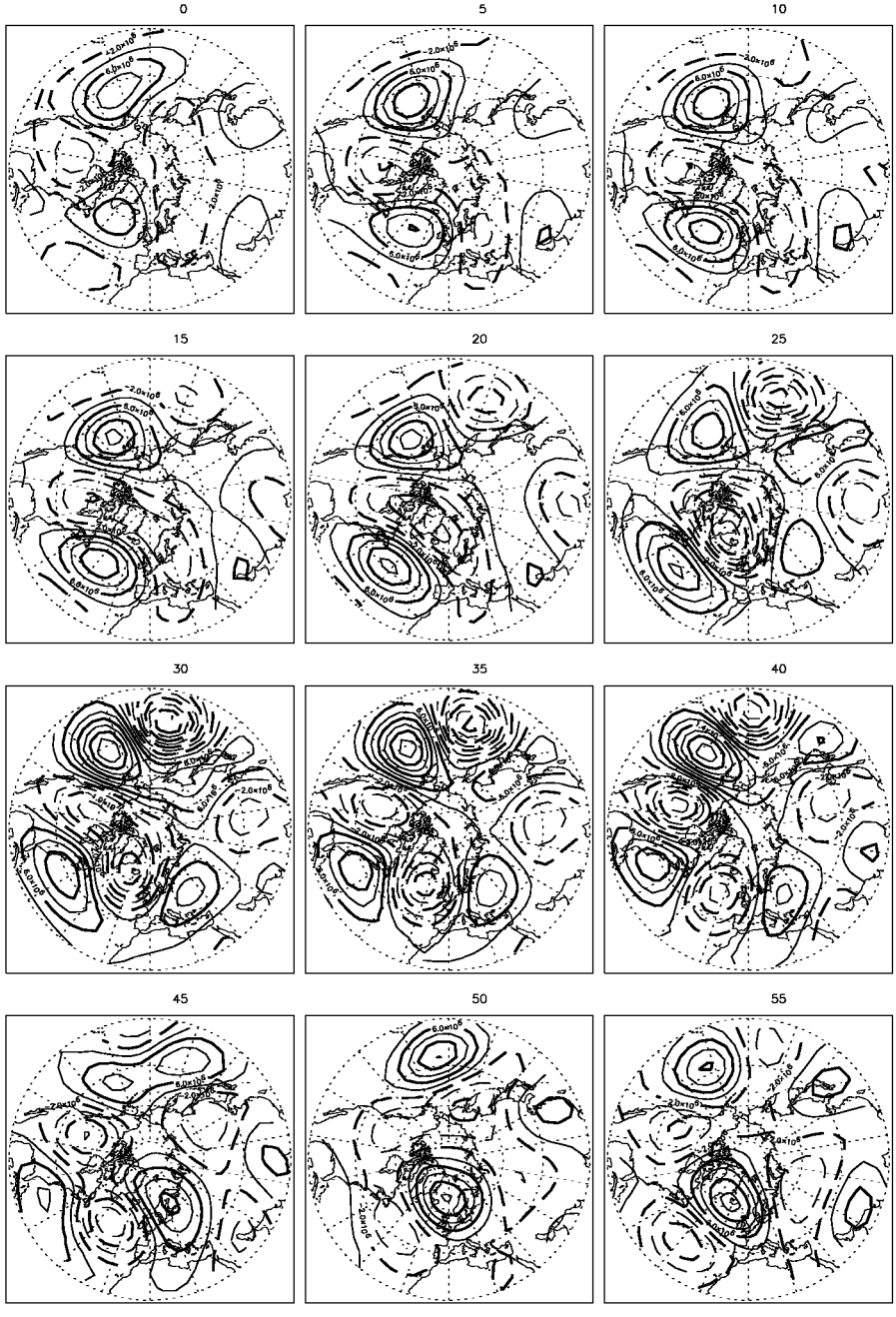

Figure 6. As in Fig. 4 but starting from the negative teleconnection state.

5. Discussion and conclusion

In this paper, the low-dimensional model developed in Part 1 has been used as a tool to study the low-frequency dynamics of the reference model.

First of all, the regimes obtained by cluster analysis in Part 1 were compared to the global quasi-equilibria of the low-dimensional model. Three of the five hemispheric regimes were found to be approximately identifiable with quasi-stationary states. One of these equilibria was found to be actively maintained by the transient part of the forcing term. The mean part of the forcing seemed sufficient to maintain the other two.

Secondly, the directions of linear instability of the quasi-stationary states have been analysed, giving information on the mechanisms of regime decay. It was found that the negative persistent anomaly over the Pacific ocean, linked to episodes of positive PNA phases, or to the state called Arctic High, is destabilized by a barotropically unstable Rossby wave propagating from the Asian continent. Another very slowly growing oscillatory mode was found in the Atlantic part of both the Negative and the Positive Teleconnection states, although with different periodicity in the two cases. This oscillatory instability suggests the existence of an oscillation between the two phases of NAO.

Although the existence of global quasi-stationary states is found in the model, the linkage of these with weather regimes is still a point that needs to be clarified. An approximate correspondence between the two was presented by Reinhold and Pierrehumbert (1982). Their model was a very simple QG channel model, with a severe truncation on the harmonic spectrum that retained 20 degrees of freedom. The correspondence between the regimes and the stationary solution was only approximate, in the sense that the time-dependent regimes normally exhibited less pronounced wave amplitudes; the authors showed that the extra forcing due to the effect of high-frequency transients was responsible for the modification of the regimes. The extension of the results of Rehinold and Pierrehumbert (1982) to more complex GCMs is made difficult by the complexity of the system of equations to be solved, so that generally no truly stationary solutions are found. Among attempted solutions of this problem, the recent work of Hannachi (1997) is quite successful; it uses the method of minimizing the barotropic potential-vorticity tendency, but projecting it on the EOFs of a GCM output. This produces resemblance between the solutions found and the regimes obtained by some form of cluster analysis of the GCM output. Nevertheless, the equation solved in this EOF subspace is not the equation of the GCM.

The present paper also uses an approach somewhat similar to Hannachi (1997). Instead of complicating a simple model, a relatively complex model is simplified, and quasi-stationary solutions are found. The difference is that here the (quasi-) stationary solutions are found on the same model equations as the complete model.

It is found that the link between weather regimes and global equilibria is not trivial. In Part I weather regimes were defined as hemispheric clusters, which allows ease of comparison with the global stationary solutions of this paper. Nevertheless, there are hints in the literature that weather regimes are better regarded as regional phenomena. Consequently, one should probably think in terms of global equilibria creating the dynamical conditions (e.g. the position of stormtracks) for the formation of local phenomena. For example, one may think that the persistence of a negative phase of the NAO may increase the probability of Euro-Atlantic blocking. In other words the regimes do not identify directly with global equilibria. Other studies, such as Hannachi (1997), and also DaCosta and Vautard (1998), have found an identity between regimes and equilibria, but at the regional scale.

Although the present work is carried out in a pure ‘perfect’ model approach, there is the clear possibility of extending the low-order model approach to the simulation of the

real atmosphere. The low-order model is composed of a dynamical part, that is basically the reduced version of a pre-existing model, and of an empirical part. The empirical part can be fitted from observed data rather than from reference-model integration, and a model of the real atmosphere can be built. Of course, this is not straightforward due to the data sampling problem. An approach in this sense was carried out by DaCosta and Vautard (1998), but with a completely empirical model.

There are good hopes of success by the use of such a model. In fact there is a remarkable resemblance between the quasi-stationary solutions of the low-order model and the weather regimes of the observed circulation that can be found in the literature; for example both Cheng and Wallace (1993) and Corti *et al.* (1999) found, with different techniques, regimes very similar to the quasi-stationary solutions of the low-order model. In the case of the Positive Teleconnection state the correspondence is even more striking. Also Shutts (1987) shows a pattern called 'severe winter' that is remarkably similar to the Arctic High state.

Oscillations with a comparable time-scale to that found in the low-order model, and characterized by westward travelling waves, have already been found in observed data (Branstator 1987; Kushnir 1987; Ghil and Mo 1991; Plaut and Vautard 1994) or GCMs (Markus *et al.* 1996). These works all use some kind of advanced space–time filtering technique, such as complex or extended EOF analysis or Singular Spectrum Analysis (SSA). Using multi-channel SSA (see Plaut and Vautard 1994 and references therein for a description) Michelangeli and Vautard (1998) found a westward travelling wave of hemispheric scale in the very same QG reference model used in this article. The same technique was also applied in this paper to the North Atlantic sector, and an oscillation closely resembling the low-order model oscillating mode of section 4(c) was found (not shown).

The analysis of such oscillations may throw some light on the existence of preferential 'paths' of variability between the different regimes, hypothesized in past studies such as Vautard *et al.* (1990) and Kimoto and Ghil (1993).

Acknowledgements

This work was partly carried out while the author was affiliated to the Institute of Geophysics and Planetary Physics (IGPP) of the University of California, Los Angeles (UCLA).

The author wishes to thank Robert Vautard, Michael Ghil, Francois Lott, Glenn Shutts and Robert Miller for interesting discussions and suggestions. An anonymous referee made a very thorough review that improved the paper. This work was partially supported by the EC project POTENTIALS (ENV4-CT97-0497) and the NSF grant ATM-0082131, via UCLA's IGPP.

References

Branstator, G. 1987 A striking example of the atmosphere's leading traveling patter. *J. Atmos. Sci.*, **44,** 2310–2323

Charney, J. G. and DeVore, J. G. 1979 Multiple flow equilibria and blocking. *J. Atmos. Sci.*, **36,** 1205–1216

Cheng, X. and Wallace, J. M. 1993 Cluster analysis of the northern hemisphere wintertime 500 hPa height field: Spatial patterns. *J. Atmos. Sci.*, **50,** 2674–2696

Corti, S., Molteni, F. and Palmer, T. N. 1999 Signature of climate change in atmospheric circulation regime frequencies. *Nature*, **398,** 799–802

Da Costa, E. and Vautard, R. 1998 A qualitatively realistic low-order model of the extratropical low-frequency variability built from long records of potential vorticity. *J. Atmos. Sci.*, **55,** 1064–1084

D'Andrea, F. and Vautard, R. 2001 Extratropical low-frequency variability as a low-dimensional problem. I: A simplified model. *Q. J. R. Meteorol. Soc.*, **127,** 1357–1374

Ghil, M. and Mo, K. 1991 Intraseasonal oscillation in the global atmosphere. Part 1: Northern hemisphere and the tropics. *J. Atmos. Sci.*, **48,** 752–779

Haines, K. and Hannachi, A. 1995 Weather regimes in the Pacific from a GCM. *J. Atmos. Sci.*, **52,** 2444–2462

Hannachi, A. 1997 Weather regimes in the Pacific from a GCM. Part II: Dynamics and stability. *J. Atmos. Sci.*, **54,** 1334–1348

Kimoto, M. and Ghil, M. 1993 Multiple flow regimes in the northern hemisphere winter. Part II: Sectorial regimes and preferred transitions. *J. Atmos. Sci.*, **50,** 2625–2643

Kushnir, Y. 1987 Retrograding wintertime low-frequency disturbances over the north Pacific Ocean. *J. Atmos. Sci.*, **44,** 2727–2742

Markus, S. L., Ghil, M. and Dickey, J. O. 1996 The extratropical 40-day oscillation in the UCLA general circulation model. Part II: Spatial structure. *J. Atmos. Sci.*, **53,** 1993–2014

Marshall, J. and Molteni, F. 1993 Towards a dynamical understanding of planetary-scale flow regimes. *J. Atmos. Sci.*, **50,** 1792–1818

Michelangeli, P. A. and Vautard, R. 1998 The dynamics of Euro-Atlantic blocking onsets. *Q. J. R. Meteorol. Soc.*, **124,** 1045–1070

Michelangeli, P. A., Vautard, R. and Legras, B. 1995 Weather regimes: Recurrence and quasi-stationarity. *J. Atmos. Sci.*, **52,** 1237–1256

Plaut, G. and Vautard, R. 1994 Spells of low-frequency oscillations and weather regimes in the northern hemisphere. *J. Atmos. Sci.*, **51,** 210–236

Reinhold, B. and Pierrehumbert, R. T. 1982 Dynamics of weather regimes: Quasi stationary waves and blocking. *Mon. Weather Rev.*, **110,** 1105–1145

Shutts, G. 1987 Persistent anomalous circulation and blocking. *Meteorol. Mag.*, **116,** 117–124

Simmons, A. J., Wallace, J. M. and Branstator, G. W. 1983 Barotropic wave propagation and instability, and atmospheric teleconnection patterns. *J. Atmos. Sci.*, **40,** 1363–1392

Vautard, R., Mo, K. C. and Ghil, M. 1990 Statistical significance test for transitional matrices of atmospheric Markov chains. *J. Atmos. Sci.*, **47,** 1926–1931